Aggregation Behaviour and Zn^{2+} Binding Properties of Secretin†

Katharine A. Carpenter*,‡ and Peter W. Schiller

Laboratory of Chemical Biology and Peptide Research, Clinical Research Institute of Montreal, 110 Pine Avenue West, Montreal, Quebec, Canada H2W 1R7

Received March 26, 1998; Revised Manuscript Received July 1, 1998

ABSTRACT: Dynamic light scattering measurements were carried out on secretin in aqueous solution (2 mM; pH 5.0). The results indicated that the molecule exists as a fairly compact hexamer under these solution conditions. Secondary structural properties of the secretin hexameric complex were evaluated using CD and NMR spectroscopy. Specifically, the spectral properties of secretin in water were examined as a function of peptide concentration. Results from the analyses indicated a 2-fold increase (17−32%) in α-helical content within the region Ser^{11}−Arg^{21} as the peptide concentration was increased from 0.1 to 2 mM. Displacement of the αH proton chemical shifts relative to random coil values did not alter significantly with increasing peptide concentration. This observation confirmed that the length of the helical segment is independent of peptide concentration between 0.1 and 2 mM. The nature of the helix was furthermore determined as amphipathic, and thus the potential for a cooperative intermolecular association through the apolar helical face of individual monomers was indicated. These findings suggest that secretin aggregates into symmetric hexamers at millimolar concentrations and, furthermore, that the helical domain is stabilized through this intermolecular association. The potential for secretin to bind divalent cations, including Ca^{2+} and Zn^{2+}, was also examined by CD[1] and NMR spectroscopy. The results revealed that Zn^{2+} specifically coordinates to the His^1 and Asp^3 residues of each secretin monomer without disrupting the peptide's helical structure, whereas Ca^{2+} did not exhibit any interaction with the peptide hormone. It was concluded from these studies that secretin may be stored in a hexameric form within its secretory tissues and that zinc may play a role in the storage of secretin through a specific interaction with the N-terminal histidine and aspartic acid residues.

Secretin is a 27-residue gastrointestinal polypeptide hormone which plays a major role in the regulation of pancreatic exocrine secretion (*1*, *2*). It is a member of the glucagon superfamily (*3*) which also includes the vasoactive intestinal peptide, gastric inhibitory peptide, and growth hormone releasing factor. The primary structure of secretin is identical to that of glucagon in 14 of the 27 amino acid residue positions (Figure 1).

Based on similarities in their primary structures, it is expected that both glucagon and secretin may be characterized by similar conformational features in solution. NMR and CD spectroscopic investigations have been carried out on the two hormones under a variety of solution conditions in order to pinpoint regions of conformational order which might be important for their biological functions (*4*−*6*). A general conclusion from these studies is that the two hormones are essentially disordered in aqueous solution at micromolar concentrations but adopt a significant amount of amphipathic helical structure in nonaqueous solvent media.

Glucagon **HSQGTFTSDYSKYLDSRRAQDFVQWLMNT-OH**

Secretin **HSDGTFTSELSRLRDSARLQRLLQGLV-NH_2**

FIGURE 1: Comparison of the amino acid sequence of glucagon with that of porcine secretin. Amino acids common to both peptides are indicated by boldface type.

At higher peptide concentrations (>1 mg/mL), glucagon readily undergoes peptide aggregation in aqueous solution accompanied by an increase in α-helical content (*7*). Based on results from sedimentation equilibrium experiments, it has been suggested that this aggregation may be described as a two-state equilibrium involving dimers and hexamers (*8*). The X-ray structure of glucagon crystallized under basic conditions is also oligomeric in nature. However, in this case, the hormone forms trimers through an intermolecular head-to-tail association involving the Phe^6, Tyr^{10}, and Tyr^{13} residues of one glucagon molecule and the Trp^{25}, Leu^{26}, and Phe^{22} residues of a second glucagon molecule (*9*). Furthermore, each glucagon molecule in the trimer adopts a helical structure encompassing residues 6−26.

The potential for secretin to self-associate into regular higher molecular weight aggregates has not yet been explored. Understanding the molecular architecture adopted by the hormone at millimolar concentration may provide

† Supported by research grants from the National Science and Engineering Research Council of Canada (to K.A.C.) and the Medical Research Council of Canada (Grants MT-5655 and MT-10131) (to P.W.S.).

* To whom correspondence should be addressed.

‡ Present address: ASTRA Research Centre Montreal, 7171 Frederick-Banting, Saint-Laurent, Montreal, Quebec, Canada H4S 1Z9. Phone: (514) 832-3200, ext 2441. FAX: (514) 832-3232. E-mail: katharine.carpenter@arcm.ca.astra.com.

[1] Abbreviations: NMR, nuclear magnetic resonance; CD, circular dichroism; DQF-COSY, double quantum filtered correlated spectroscopy; TOCSY, total correlation spectroscopy; NOESY, nuclear Overhauser enhancement spectroscopy; TSP, 3,3,3-trimethylsilylpropionate; ms, millisecond(s).

10.1021/bi980701x CCC: $15.00
Published on Web 11/11/1998

important insight into the molecular form in which the hormone exists within in its storage/secretory tissues. Insulin, for example, is known to self-associate into hexamers in the presence of divalent metal ions (*10*). It is believed that this metal-dependent association contributes to peptide stability within the secretory/storage granules of the pancreatic islet cells (*11*). The purpose of the present study was to determine whether secretin remains monomeric and disordered in water over a broad concentration range or readily associates into structurally uniform aggregates at higher concentrations. The hormone's ability to bind Zn^{2+} or Ca^{2+} was also examined.

MATERIALS AND METHODS

Porcine secretin (pentachloride form) was a generous gift from Dr. J. Knolle (Hoechst AG, Frankfurt am Main, FRG).

Circular Dichroism Spectroscopy. Samples for CD spectroscopy were prepared by diluting a 2 mM stock solution of secretin in 50 mM sodium phosphate buffer (pH 6.0) with measured aliquots of the same buffer. The resulting four samples had concentrations of 0.1, 0.5, 1, and 2 mM, respectively, and a pH of 5.0. CD spectra were recorded on a JASCO J710 spectropolarimeter operating at room temperature (22 °C). Eight scans were collected for each sample over a wavelength range of 184−260 nm, using a 0.01 cm path length cell, a 100 mdeg sensitivity, a 0.2 nm resolution, a 1.0 nm bandwidth, a 100 nm/min scan speed, and a 0.25 s response time. The collected spectra were subjected to background subtraction and smoothing and then were converted to units of molar ellipticity per residue (deg cm^2 $dmol^{-1}$). The degree of α helicity was determined from the intensity of the ellipticity at 222 nm using the Chen method of analysis (*12*). For zinc binding studies, aliquots of either a 1.7 mM or a 33 mM stock solution of $ZnCl_2$ in Tris buffer (50 mM; pH 7.15) were added to six different dilute secretin samples in the same buffer. A Tris rather than phosphate buffer was employed for these experiments since the formation of insoluble zinc−phosphate complexes was found to occur when Zn^{2+} was added to solutions of secretin in phosphate buffer. The sample volumes were adjusted such that the concentration of peptide was 40 μM in each sample and the concentration of zinc varied from 0 to 1.2 mM. CD spectra were acquired for the samples using the same acquisition parameters described above and a 0.1 cm path length cell. For the Ca^{2+} binding studies, 1.6 mg of $CaCl_2$ was added to 500 μL of a secretin sample in 50 mM Tris buffer (pH 7.15) such that the final concentrations of peptide and Ca^{2+} were 40 μM and 29 mM, respectively. A CD spectrum was acquired for this sample using a 0.1 cm path length cell.

The conformational stability of secretin was assessed from the temperature dependence of CD spectra acquired for 2 mM secretin at 5 °C intervals between 20 and 50 °C. Thermal destabilization was indicated by a change in absorbance at 222 nm.

Dynamic Light Scattering. The secretin sample for dynamic light scattering measurements was prepared by dissolving 3.1 mg of peptide in 500 μL of 50 mM phosphate buffer (pH 6.0). This resulted in a peptide sample concentration of 2 mM and a sample pH of 5.0. Measurements were made on a DynaPro-801 Dynamic Light Scattering Instrument operating at 20 °C. The scattered light intensity was collected at regular intervals over a period of 12 min, resulting in a total of 16 useful measurements, and the accumulated data were fit to a monomodal (single Gaussian) distribution. The translational molecular diffusion coefficient, Stoke's radius, and molecular weight were calculated from the autocorrelated scattered light intensity data, using standard equations (*13*).

NMR Spectroscopy. Aqueous samples of secretin employed for metal binding experiments were prepared by adding 3.1 mg of peptide to 500 μL of 30 mM sodium acetate buffer (90% H_2O/10% D_2O; pH 6.0). Samples of secretin used for additional NMR experiments contained 0.8, 1.6, 3.1, or 4.7 mg of peptide dissolved in 500 μL of 50 mM sodium phosphate buffer (90% H_2O/10% D_2O; pH 6.0). The sample pH was adjusted to 5.0 with dilute NaOD in all cases. All NMR spectra were recorded on a Bruker DMX-600 spectrometer at 30 °C unless indicated otherwise. Proton chemical shift assignments were made using standard procedures (*14*). Spin systems of individual amino acids were first identified from DQF-COSY (*15*) and TOCSY (*16*) data sets. Completion of the sequential assignment then proceeded through analysis of a 2D NOESY (*17*) spectrum acquired for the sample. Mixing times of 50 and 100 ms were employed for the TOCSY and NOESY experiments, respectively. The 2D spectra were acquired in the phase-sensitive mode, using either the TPPI or the States-TPPI method, and typically were 512 data points in F1 and 2K data points in F2 with spectral widths of 6000 Hz in each dimension. Phase-shifted sine-squared window functions were applied along both dimensions prior to Fourier transformation. Gradient water suppression was achieved by using the WATERGATE technique (*18*). Chemical shifts were referenced indirectly to 3,3,3-trimethylsilylpropionate (TSP).

Secretin was found to be completely insoluble at millimolar concentrations when the sample pH was raised above pH 5.0, indicating that one ionizable group in the molecule must have a pK_a around pH 5.0. The chemical shifts corresponding to the side chain β protons of the four acidic residues in secretin were therefore monitored as a function of sample pH. Results of this pH titration are shown in Figure 2. It is clear from the titration curves that Asp^3, Asp^{15}, and Glu^9 all have pK_a values in the normal range for these residues, i.e., between pH 3 and pH 4. The His^1 group, however, has a pK_a in the vicinity of pH 5, and it is therefore this residue which is responsible for the solubility of the peptide below pH 5.

Temperature coefficients for the backbone amide protons and εNH of each arginine side chain were determined by measuring their associated ^1H chemical shifts at 5 °C intervals between 10 and 35 °C. The chemicals shifts were referenced relative to their starting values at 10 °C. Plots of chemical shifts vs temperature were linear in all cases, suggesting that major conformational transitions did not occur in this temperature range.

For the Zn^{2+} ion titration study, aliquots of a 33 mM stock solution of $ZnCl_2$ were added to a 2 mM aqueous sample of secretin in acetate buffer (pH 5.0), and a 1D ^1H NMR spectrum was acquired after each addition. The binding affinity of secretin for Ca^{2+} was examined by adding a 5 molar equiv excess of $CaCl_2$ to a 2 mM aqueous sample of

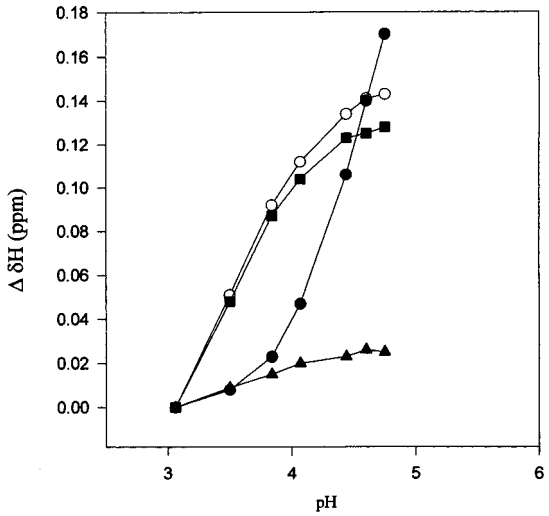

FIGURE 2: Chemical shift variation of the C_2H proton for His[1] (solid circles), and of β protons of residues Asp[3] (open circles), Glu[9] (triangles), and Asp[15] (squares) during a pH titration of 2 mM secretin in H_2O.

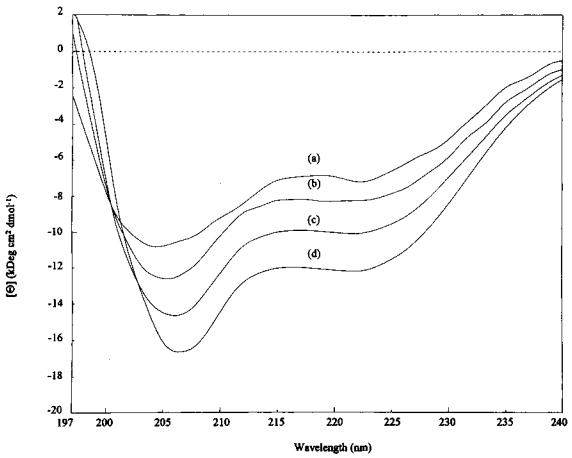

FIGURE 3: Circular dichroism spectra of secretin in aqueous solution at 22 °C and at different concentrations: (a) 0.1 mM, (b) 0.5 mM, (c) 1 mM, and (d) 2 mM.

secretin, and a 1D ^{1}H NMR spectrum was acquired for the sample immediately before and 24 h after addition of the salt.

RESULTS

CD Studies. Figure 3 depicts CD spectra of secretin collected at four different peptide concentrations. Double minima are observed at approximately 208 and 222 nm in all four spectra, indicating the presence of helical structure. Upon changing the peptide concentration from 0.1 to 2 mM, the circular dichroism spectrum underwent changes which reflected a progressive increase in helix formation (Figure 3). The degree of molecular helicity calculated from the molar ellipticity at 222 nm (*12*) increased with increasing peptide concentration, exhibiting limiting values of 17% and 32% for the 0.1 and 2 mM secretin samples, respectively. It is clear from these CD spectral changes, occurring as a result of varying the secretin concentration, that the peptide hormone exists as a molecular aggregate in aqueous solution. The fact that the helical content increased with increasing peptide concentration suggests that the helical structure is stabilized through intermolecular association.

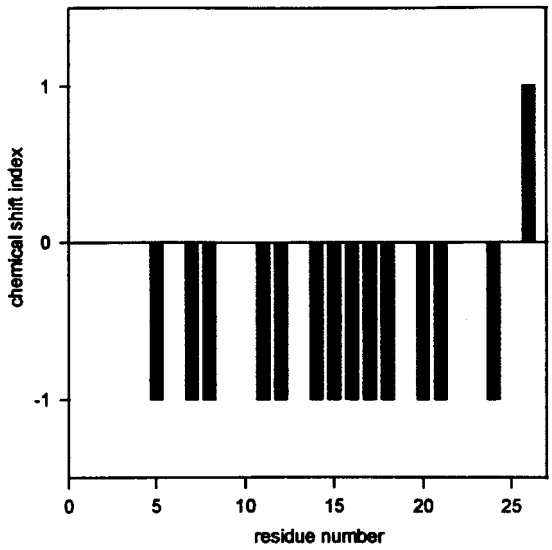

FIGURE 4: Chemical shift index of αH protons for 2 mM secretin in H_2O (30 °C) [see (*19*) for details of the analysis].

Light Scattering. Dynamic light scattering measurements carried out on a 2 mM secretin sample at 20 °C yielded valuable information concerning the aggregation state of the peptide in water. A total of 16 measurements were recorded, and the average translational diffusion coefficient (D_T), Stoke's radius (R_S), estimated molecular weight, and sample polydispersity were determined from the results. The measured polydispersity (2.07 Å) was less than 15% of the estimated Stoke's radius ($R_S = 21.24$ Å), indicating that the secretin sample was monodisperse. This result provides confirmatory evidence that secretin exists predominantly as a single molecular weight aggregate in aqueous buffer at 2 mM concentration, pH 5.0 and 20 °C. The estimated molecular mass consistently returned from each dynamic run was 18 kDa, which is 6 times the molecular mass of the secretin monomer. Thus, secretin associates as a hexamer in aqueous solution.

NMR Studies. ^{1}H NMR experiments were initially carried out on the 2 mM sample of secretin at 25 °C. A single set of proton resonances was assigned to each residue in the sequence, and, furthermore, this feature did not change upon lowering the sample temperature to 15 °C or increasing it to 35 °C. This result suggests that the six secretin molecules within each hexamer are interacting in a symmetric fashion. Any asymmetry would introduce a range of chemical shift environments for protons directly involved in the intermolecular association, and, hence, additional peaks or severe selective line-broadening would be observed in the ^{1}H NMR spectra.

Residues contributing to the α-helical region of secretin were identified using the chemical shift indexing method described by Wishart and co-workers (*19*). The α proton chemical shift value for each residue in secretin was compared to its random coil counterpart (αH_R) statistically determined from an extensive database of protein structures (*19*). If $\alpha H\text{-}\alpha H_R > 0.1$ ppm, then that residue was assigned an index of 1. Conversely, if $\alpha H\text{-}\alpha H_R < -0.1$ ppm, then the residue was indexed as −1. A minimum of four consecutive −1's not interrupted by a 1 defines an α-helical region. Application of this method to the 2 mM sample of secretin yielded the index values shown in Figure 4.

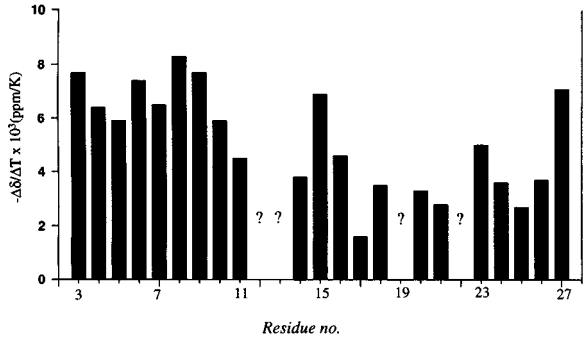

FIGURE 5: Amide proton temperature coefficients for 2 mM secretin in H_2O (30 °C). Protons for which chemical shift changes could not be assigned unambiguously due to spectral overlap are indicated by question marks.

Apparent in Figure 4 is a large density of −1's and a total absence of 1's in the region Ser^{11}−Arg^{21}, indicating that this segment of secretin is primarily α-helical. The same chemical shift analysis was repeated for three additional NMR samples with secretin concentrations of 0.5, 1, and 3 mM, respectively. Identical sets of α proton index values were obtained for all four peptide concentrations, suggesting that it is not the number of residues involved in the α-helix that is changing but rather the proportion of the secretin conformational ensemble adopting α-helical structure which is becoming larger with increasing peptide concentration. It is interesting to note that residues Ser^{11}−Arg^{21} represent 37% of the entire peptide sequence, a result which is in close agreement with the value of 32% molecular helicity determined from the CD measurements with the 2 mM secretin sample. The fact that at a peptide concentration of 2 mM the percent helicity calculated from the CD measurements approaches the percentage of residues adopting α-helical structure indicated by the NMR data suggests that at this concentration the region encompassing residues Ser^{11}−Arg^{21} in secretin is already predominantly α-helical.

The presence of intramolecular hydrogen bonding involving the backbone amide protons and arginine side chain NH protons was evaluated by examining the shifts of the NH protons relative to a starting value, with respect to temperature. Temperature coefficients calculated from linear plots of the arginine ϵNH proton chemical shift vs temperature (10^3 ppm/K) were 3.8, 5.8, 3.4, and 2.9 for Arg^{12}, Arg^{14}, Arg^{18}, and Arg^{21}, respectively. Temperature coefficients measured for the backbone amide protons are displayed in Figure 5.

A number of strong sequential $d_{NN}(i,i+1)$ NOEs were observed within the region of secretin proposed to adopt a helical structure (Ser^{11}−Arg^{21}). These include $d_{NN}(i,i+1)$ NOEs between Leu^{10} and Ser^{11}, Arg^{14} and Asp^{15}, Ser^{16} and Ala^{17}, and between Ala^{17} and Arg^{18}. There were also several additional $d_{NN}(i,i+1)$ NOEs which could not be distinguished due to spectral overlap. For example, there was a strong $d_{NN}(i,i+1)$ NOE cross-peak that was assigned to three different pairs of sequential residues including Leu^{13} and Arg^{14}, Leu^{19} and Gln^{20}, and Gln^{20} and Arg^{21}. In other cases, degenerate resonance frequencies associated with sequential amide protons such as those belonging to Arg^{18} and Leu^{19} (Table 1) prevented observation of the corresponding $d_{NN}(i,i+1)$ NOEs.

In support of a helical structure, a $d_{\beta N}(i,i+3)$ NOE between Ala^{17} and Gln^{20} was observed. There were also three other cases where an NOE cross-peak appeared between protons expected to be close together in a helical structure but were interpreted with caution due to spectral overlap and the aggregated nature of the peptide. These included $d_{\alpha N}(i,i+3)$ and $d_{\beta N}(i,i+3)$ NOEs between Asp^{15} and Arg^{18} and a $d_{\beta N}(i,i+4)$ NOE connecting Glu^9 and Leu^{13}. Spectral crowding in the αH−NH region of the NOESY spectrum prevented assignment of other medium-range NOEs involving residues in the proposed helical region of secretin.

Table 1: ^{1}H Chemical Shifts (ppm) of 2 mM Secretin in H_2O at 303 K[a]

residue no.	NH	αH	βH	other
His^1			3.28	C_2H 8.53; C_4H 7.35
Ser^2		4.56	3.86	
Asp^3	8.64	4.68	2.74, 2.71	
Gly^4	8.41	3.97		
Thr^5	8.06	4.13	4.26	γCH_3 1.10
Phe^6	8.37	4.67	3.06, 3.17	
Thr^7	8.02	4.21	4.21	γCH_3 1.19
Ser^8	8.29	4.39	3.89, 3.99	
Glu^9	8.49	4.21	2.03, 2.32	
Leu^{10}	8.09	4.17	1.62, 1.65	δCH_3 0.83, 0.90; γH 1.56
Ser^{11}	8.20	4.27	3.94, 3.98	
Arg^{12}	7.96	4.22	1.60, 1.67	δCH_2 3.19; NH 7.30; γCH_2 1.83, 1.90
Leu^{13}	7.96	?[b]		δCH_3 0.86, 0.90
Arg^{14}	8.12	4.16	1.62, 1.72	δCH_2 3.20; NH 7.25; γCH_2 1.88
Asp^{15}	8.20	4.59	2.74, 2.71	
Ser^{16}	8.07	4.24	3.90, 3.95	
Ala^{17}	8.22	4.23	1.47	
Arg^{18}	7.97	4.09	1.57, 1.70	δCH_2 3.23; NH 7.33; γCH_2 1.88
Leu^{19}	7.96	?		δCH_3 0.86, 0.90
Gln^{20}	8.14	4.06	2.10	γCH_2 2.37, 2.44
Arg^{21}	7.94	4.16	1.61, 1.72	δCH_2 3.18; NH 7.22; γCH_2 1.85, 1.90
Leu^{22}	7.96	?		δCH_3 0.86, 0.90
Leu^{23}	8.12	4.20	1.72	δCH_3 0.83, 0.88; γH 1.59
Gln^{24}	8.05	4.21	2.10	γCH_2 2.40, 2.45
Gly^{25}	8.10	3.94		
Leu^{26}	7.89	4.35	1.67, 1.70	δCH_3 0.85, 0.89; γH 1.58
Val^{27}	7.88	4.07	2.09	0.94

[a] ^{1}H chemical shifts are referenced to 3,3,3-trimethylsilylpropionate (0 ppm). [b] ?: α proton chemical shift is either 4.16 or 4.23 ppm.

The stability of the helical structure was determined by comparing CD spectra obtained for 2 mM secretin at different temperatures between 20 and 50 °C. There was no change observed in the CD spectrum acquired for secretin when the sample temperature was in the range 20−45 °C. A slight decrease in the absorbance at 222 nm was observed when the sample temperature was raised to 50 °C, indicating the onset of thermal destabilization of the hexamer structure at this temperature.

Metal Binding Experiments. The ability of secretin to bind divalent cations under conditions in which the peptide is solubilized at high concentration (2 mM) or low concentration (40 μM) was explored using NMR and CD spectroscopy. Titration of an aqueous 2 mM sample of secretin (pH 5.0) with Zn^{2+} resulted in spectral changes occurring for several of the ^{1}H resonances of residues in the N-terminal region of the molecule (Figure 6). These included upfield chemical shift displacements of the Gly^4 NH and the His^1 C_4H and β protons, a downfield shift of the Asp^3 β proton resonances, and a collapse of the multiplet associated with the two Ser^2 β protons, as the Zn^{2+}:peptide concentration ratio increased from 0:1 to 3:1. Conversely, there were no NMR spectral changes observed when excess $CaCl_2$ was added to a 2 mM sample of secretin at pH 5.0 even 24 h after addition of the

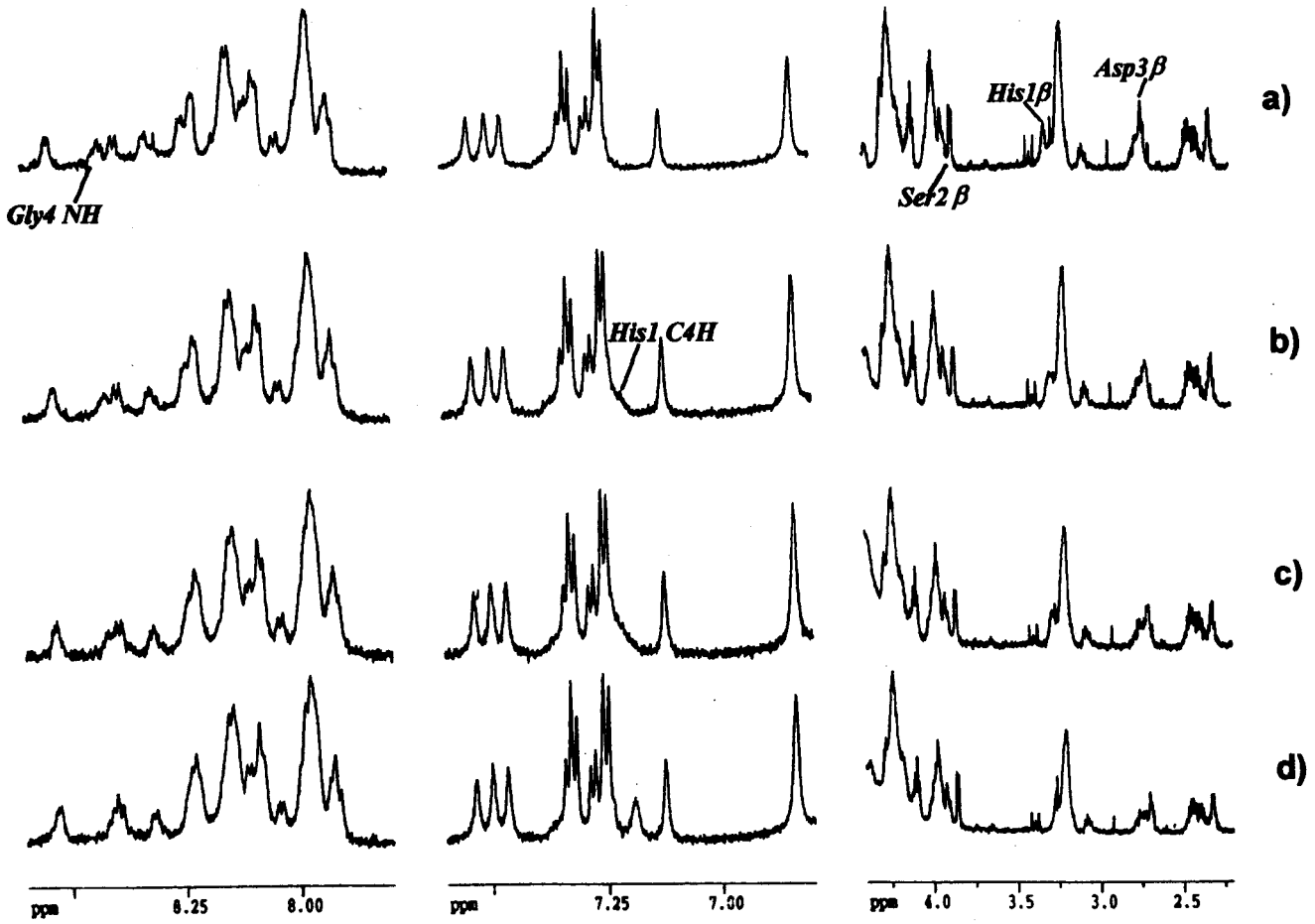

FIGURE 6: ^{1}H NMR spectra for 2 mM secretin in H_2O containing $ZnCl_2$ at Zn^{2+}:secretin concentration ratios of (a) 0:1, (b) 1:1, (c) 2:1, and (d) 3:1.

metal. Metal binding studies were repeated for secretin at low concentration (40 μM; pH 7.15) where the peptide is expected to exist in its monomeric form. Under these dilute conditions, secretin still adopts some partial helical structure, as evidenced by the CD spectrum acquired for the peptide in the absence of metal. Addition of Zn^{2+} to the sample did not produce significant changes to the CD spectrum, suggesting that binding of Zn^{2+} to the secretin monomer does not significantly affect the helical structure of the molecule.

DISCUSSION

Early circular dichroism studies carried out on secretin revealed that the molecule contains some partial helical structure in dilute aqueous solution (*20*). The amount of secretin helical structure was later shown to increase dramatically in the presence of anionic lipids (*4*). Helical propagation probability calculations performed on secretin indicated that the helical region lies within residues Leu^{13}−Gln^{20} (*4*). This prediction is in close agreement with the Ser^{11}−Arg^{21} helical region determined in the present study. Segrest and co-workers (*21*) classified the originally proposed α-helical region (residues 13−20) of secretin as a class H amphipathic helix on the basis of the molecule's hormonal properties and high density of positive charge. Incorporating amino acids Leu^{10}−Arg^{21} of secretin into a helical wheel diagram (Figure 7) demonstrates that extending the helical region of secretin to include residues Leu^{10}−Arg^{21} does not affect the amphipathic nature of the helix. Four positively

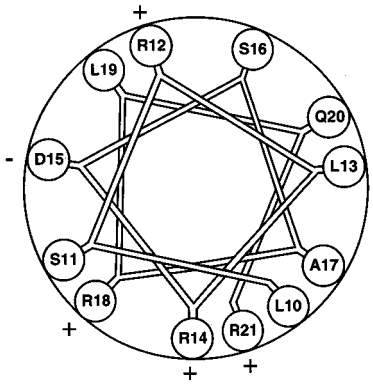

FIGURE 7: Helical wheel diagram of secretin in the region Leu^{10}−Arg^{21}.

charged arginines and a negatively charged Asp^{15} are now located on the hydrophilic face of the amphipathic helix, while Ala^{17}, Leu^{13}, and possibly Leu^{10}, which resides at the edge of the helical region, make up the hydrophobic face of the peptide.

The dependence of the amide proton chemical shifts on temperature was consistently lower in the region Ser^{11}−Leu^{26} than in the region Asp^{3}−Leu^{10} (Figure 5). This suggests that amide protons in the proposed helical region (Ser^{11}−Arg^{21}) are comparatively more shielded from the aqueous solvent than those within the N-terminal segment Asp^{3}−Leu^{10}. Reduced amide proton solvent exposure found to occur for residues Ser^{11}−Arg^{21} is likely a consequence of intramolecular hydrogen bonding between amide protons and

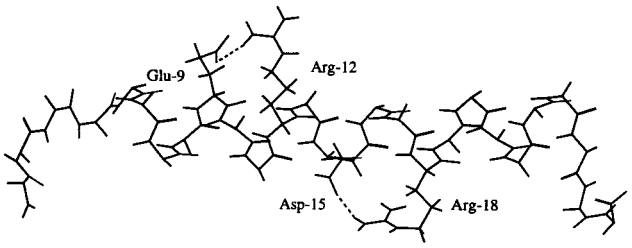

FIGURE 8: Model of a secretin monomer containing a helical structure from Ser^{11} through Arg^{21}. Sites of interresidue salt bridges are illustrated by dotted lines.

backbone carbonyls involving these residues. This finding is consistent with a high population of helical structure within the region $Ser^{11}-Arg^{21}$ of secretin. There was one residue in the proposed helical region (Asp^{15}) for which a slightly higher amide proton temperature coefficient was obtained. It is therefore possible that a slight bend in the helical structure occurs at residue 15. Low ϵNH temperature coefficients were also obtained for three out of the four arginine residues: Arg^{12}, Arg^{18}, and Arg^{21}. The presence of a salt bridge between a positively charged arginine side chain and a negatively charged aspartic acid or glutamic acid side chain would explain the low degree of exposure to the aqueous environment observed for these ϵNH protons.

The potential for the side chain carboxyl group of Glu^9 or Asp^{15} to form a salt bridge with one of the cationic sites provided by the four arginine side chains was determined in a previous study by comparing the ORD spectra obtained for 9-glutamine secretin and 15-asparagine secretin with that obtained for the parent peptide (*22*). A loss of helical structure was observed in both cases presumably due to the removal of interresidue salt bridges important for stabilizing the helix. A model of secretin containing a helical structure from Leu^{10} to Arg^{21} was constructed in order to visualize potential sites of side chain interactions (Figure 8). According to the model, salt bridges are easily formed between the side chains of Asp^{15} and Arg^{18} and between the side chains of Glu^9 and Arg^{12}. Reduced exposure to the aqueous solvent experienced by the Arg^{12} and Arg^{18} ϵNH protons as a consequence of these two ionic bonds is supported by the low temperature coefficients measured for the Arg^{12} and Arg^{18} ϵNH protons. The fact that neither Glu^9 or Asp^{15} bound Ca^{2+} provides additional evidence for the presence of salt bridges involving these two residues, since calcium is known to preferentially bind to the anionic carboxylate function of aspartic acid and glutamic acid residues.

That the helical core of secretin is stabilized through intermolecular association is evident from the CD and NMR concentration dependence studies. Changes in spectral properties upon variation of the concentration were apparent in both cases (Figures 3 and Table 1). An increase in α-helical content from 17% to 32% was observed when the peptide concentration was increased from 0.1 to 2 mM. The fact that at a peptide concentration of 2 mM the amount of helical structure in secretin determined from the CD measurements agrees well with the 37% molecular helicity indicated by the NMR α proton chemical shift data suggests that the molecule is almost fully associated at this concentration. Further evidence in support of this finding is derived from results obtained from the light scattering experiments. Negligible polydispersion was observed with the 2 mM sample examined, and the obtained molecular mass of 18 kDa was indicative of a secretin hexamer. Therefore, although it is possible that lower molecular mass secretin aggregates or monomers may also be present in solution at millimolar concentration levels, their proportion must be very low.

The NOESY spectra acquired for 2 mM secretin contained numerous interresidue NOEs, indicating that the peptide adopts a well-defined structure at this concentration in aqueous solution. However, these NOEs were not used to calculate a structure for the secretin hexamer since intramolecular NOEs could not unambiguously be distinguished from intermolecular NOEs. This problem was further complicated by the large amount of spectral overlap observed to occur among the leucine and arginine residues (Table 1). Nevertheless, some general statements can be made regarding global structural features of the secretin hexamer. Both the αH chemical shifts and amide proton temperature coefficients support the presence of a helix in the region $Ser^{11}-Arg^{21}$ of secretin. The observation of strong sequential $d_{NN}(i,i+1)$ NOEs in this segment of the peptide provides further evidence for the presence of a helical structure. By contrast, NOE cross-peaks within the secretin N-terminal segment His^1-Gly^4 were extremely weak, indicating a comparatively greater flexibility for this portion of the molecule. This result is supported by the comparatively higher amide proton temperature coefficients found to occur in the N-terminal region of secretin (Figure 5). The hexamer must be symmetric since a single set of sharp resonances was observed in the proton spectra acquired for 2 mM secretin. This would only occur if all the protons in one monomer of the hexamer are in identical chemical shift environments as their counterparts in the five remaining monomeric units. It is quite possible that the secretin hexamer structure involves pairwise association between amphipathic helices located on distinct monomers within the hexamer. If the apolar faces of two helices are in fact associating, then they must be doing so in a parallel or tilted parallel fashion since long-range NOEs between residues at opposite ends of the proposed helical region ($Ser^{11}-Arg^{21}$) were not observed. The experimentally determined Stokes radius for 2 mM secretin (21.2 Å) is considerably smaller than the length calculated for the extended peptide (49.06 Å), suggesting that the secretin hexamer is a fairly compact structure. Finally, the very low polydispersity obtained from light scattering measurements carried out on 2 mM secretin defines an equilibrium in which the secretin hexamer is highly favored over higher or lower molecular weight aggregates.

Several studies have demonstrated a possible link between the storage and/or function of secretin and zinc. For example, high concentrations of zinc are found in the pancreatic secretory tissues and intestinal mucosa which are sites of secretin storage and action, respectively. Secretin-induced bicarbonate output has also been shown to be greatly reduced in zinc-deficient rats (*23*). The concentration of zinc in the pancreatic tissues is significantly correlated with both endo- and exocrine function (*24*). Zinc is known to play a structural role in the storage of another hormone, insulin, produced in the β cells of the pancreatic islets (*11*). Secretin has also been shown to be transiently expressed in these insulin-producing β cells (*25*).

In the present study, the potential for secretin to bind Zn^{2+} was investigated. Based on specific ^1H chemical shift displacements, which resulted from addition of Zn^{2+} to a 2 mM sample of secretin, it can be concluded that zinc binds to the N-terminal region of the molecule. Specific residues involved in the metal binding site likely include His^1 and Asp^3 for two reasons. First of all, the proton resonances associated with these two residues and their nearest neighbors (Ser^2 and Gly^4) exhibited significant NMR spectral changes upon addition of Zn^{2+} (Figure 6), and, second, the Zn^{2+} binding amino acid side chains most frequently found in nature are the histidine imidazole and, to a lesser extent, the carboxyl of aspartic acid (or glutamic acid). Evidence for the formation of a hydrogen bond involving the Asp^3 side-chain carboxyl group and Gly^4 NH, which resulted from this metal−peptide interaction, was also obtained. In particular, an upfield chemical shift displacement of the Gly^4 NH reflecting movement of this proton to a more solvent-shielded environment was observed. A hydrogen bond of this nature is commonly seen in polypeptides and restricts the aspartic acid side chain to adopt exclusively a g(+) configuration. Addition of Zn^{2+} to the 2 mM sample of secretin did not produce any chemical shift changes in the helical portion of the hormone. This result supports the presence of two salt bridges involving Glu^9 and Asp^{15}, since the negatively charged carboxylate groups in the side chains of these two residues are not available for binding zinc. It is apparent from the Zn^{2+} titration data presented in Figure 6 that NMR signal changes continue to occur beyond a Zn^{2+}:secretin concentration ratio of 1:1. This would indicate only a moderate binding affinity of the peptide for zinc, since each secretin monomer apparently contains only one Zn^{2+} binding site. At pH 5.0, however, His^1 is only partially deprotonated (Figure 2), and therefore a considerable proportion of the secretin monomers in solution contain a positively charged N-terminal histidine side chain at pH 5. The positive charge on histidine will repel rather than attract the positively charged zinc ion. Hence, the overall observed Zn^{2+} affinity for secretin is expected to be lower when the N-terminal histidine imidazole group is in a state of equilibrium between a protonated and a deprotonated state rather than in a completely deprotonated state.

The CD data obtained for secretin under more dilute conditions (40 μM) were more difficult to interpret. There was no evidence of secondary structural changes occurring in samples containing Zn^{2+}:peptide concentration ratios of 0:1, 1:1, 3:1, 4:1, 15:1, and 30:1. It is clear from these data that the presence of zinc does not affect the helical structure of secretin at 40 μM concentration. Furthermore, the assembly of secretin into hexamers does not depend on the presence of zinc, since aggregation of the peptide into hexamers at 40 μM concentration would be expected to be accompanied by an increase in helical structure. It is possible that Zn^{2+} binds to the N-terminus of secretin at 40 μM concentration without inducing a change in the peptide's secondary structure. However, this could not be unambiguously determined from the CD spectra. Addition of a 10 molar equiv of Ca^{2+} to a 40 μM sample of secretin also did not produce any evidence of a metal−peptide interaction, since identical CD spectra were obtained for the peptide both in the presence and in the absence of calcium.

Insulin is stored as crystalline hexamers inside the secretory granules of the pancreatic β cells, coordinated by both Ca^{2+} and Zn^{2+}. Upon being released into circulation, the concentration of insulin drops dramatically from approximately 40 mM to within $10^{-9}-10^{-11}$ M, thus allowing the hexamer to dissociate into its bioactive monomeric form (*11*). In the present study, it was demonstrated that secretin associates as symmetric hexamers at millimolar concentrations. Further concentration of the hormone to levels found within secretory granules (~40 mM) (*26*) could therefore promote aggregation of secretin into a crystalline array of hexamers in a manner similar to what has previously been observed for insulin (*11*). It is not clear whether Zn^{2+} plays a role in the storage of secretin, although high concentrations of zinc are found in the duodenal mucosa. Perhaps zinc might aid in the assembly of secretin hexamers within its secretory granules via coordination of one Zn^{2+} with two His^1, Asp^3 zinc binding sites located on two distinct hexamers.

In conclusion, the results of this study show that secretin aggregates as a symmetric hexamer in aqueous solution at millimolar concentrations. The stabilization of an amphipathic α-helical structure within the peptide region Leu^{10}−Arg^{21} is furthermore promoted through this molecular self-association. It is thus possible that secretin exists as a stable hexamer when in a highly concentrated form (~40 mM) within its storage/secretory tissues and then dissociates into the bioactive monomeric form when diluted to picomolar concentrations following its release into circulation (*27*).

ACKNOWLEDGMENT

We thank Dr. Joanne Turnbull for valuable assistance with the CD measurements, Yunge Li for skilled technical assistance in carrying out the light scattering measurements, Dr. J. Knolle (Hoechst AG, Frankfurt) for donating the secretin, and Dr. Brian Wilkes for providing a model of the secretin monomer. We are also grateful to Dr. Mirek Cygler for allowing us to use the DynaPro-801 dynamic light scattering instrument at the Biotechnology Research Institute of Montreal (Canadian National Research Council). NMR spectra were obtained in the Department of Chemistry at the University of Montreal, and CD experiments were performed in the Department of Chemistry at Concordia University.

REFERENCES

1. Bayliss, W. M., and Starling, E. H. (1902) *J. Physiol. (London) 28*, 325−353.
2. Mutt, V., Jorpes, J. E., and Magnusson, S. (1970) *Eur. J. Biochem. 15*, 513−519.
3. Bell, G. I. (1986) *Peptides 7, Suppl. 1*, 27−36.
4. Robinson, R. M., Blakeney, E. W., Jr., and Mattice, W. L. (1982) *Biopolymers 21*, 1217−1228.
5. Braun, W., Wider, G., Lee, K. H., and Wüthrich, K. (1983) *J. Mol. Biol. 169*, 921−948.
6. Gronenborn, A. M., Bovermann, G., and Clore, G. M. (1987) *FEBS Lett. 215*, 88−94.
7. Srere, P. A., and Brooks, G. C. (1969) *Arch. Biochem. Biophys. 129*, 708−710.
8. Swann, J. C., and Hammes, G. G. (1969) *Biochemistry 8*, 1−7.
9. Sasaki, K., Dockerill, S., Adamiak, D. A., Tickle, I. J., and Blundell, T. (1975) *Nature 257*, 751−757.
10. Baker, E. N., Blundell, T. L., Cutfield, J. F., Cutfield, S. M., Dodson, E. J., Dodson, G. G., Hodgkin, Hubbard, R. E., Isaacs,

N. W., Reynolds, C. D., Sakabe, K., Sakabe, N., and Vijayan, N. M. (1988) *Philos. Trans. R. Soc. London 319*, 369−456.
11. Goldman, J., and Carpenter, F. H. (1974) *Biochemistry 13*, 4566−4574.
12. Chen, Y. H., Yang, J. T., and Martinez, H. M. (1972) *Biochemistry 11*, 4120−4131.
13. Harding, S. E. (1994) *Methods Mol. Biol. (Totowa, N.J.) 22*, 97−108.
14. Wüthrich, K. (1986) *NMR of Proteins and Nucleic Acids*, John Wiley and Sons, New York.
15. Rance, M., Sorensen, O. W., Bodenhausen, G., Wagner, G., Ernst, R. R., and Wüthrich, K. (1983) *Biochem. Biophys. Res. Commun. 117*, 479−485.
16. Bax, A., and Davis, D. G. (1985) *J. Magn. Reson. 65*, 355−360.
17. Jeener, J., Meier, B. H., Bachmann, P., and Ernst, R. R. (1979) *J. Chem. Phys. 71*, 4546−4553.
18. Piotto, M., Saudek, V., and Sklenar, V. (1992) *J. Biomol. NMR 2*, 661−665.
19. Wishart, D. S., Sykes, B. D., and Richards, F. M. (1992) *Biochemistry 31*, 1647−1651.
20. Bodanszky, A., Ondetti, M. A., Mutt, V., and Bodanszky, M. (1969) *J. Am. Chem. Soc. 91*, 944−949.
21. Segrest, J. P., Garber, D. W., Brouillette, C. G., Harvey, S. C., and Anantharamaiah, G. M. (1994) *Adv. Protein Chem. 45*, 303−369.
22. Bodanszky, M., Fink, M. L., Funk, K. W., and Said, S. I. (1976) *Clin. Endocrinol. 5*, 195s−200s.
23. Issoual, D., Mallet, B., Bernard, J. P., and Laugier, R. (1991) *Pancreas 6*, 330−340.
24. Kato, K., Isaji, S., Kawarada, Y., Hibasami, H., and Nakashima, K. (1997) *Pancreas 14(2)*, 158−165.
25. Wheeler, M. B., Nishitani, J., Buchan, A. M. J., Kopin, A. S., Chey, W. Y., Chang, T. M., and Leiter, A. B. (1992) *Mol. Cell. Biol. 12*, 3531−3539.
26. Hutton, J. C., Penn, E. J., and Peshavaria, M. (1983) *Biochem. J. 210*, 297−305.
27. Sanchez-Vicente, C., Rodriguez-Nodal, F., Minguela, A., Garcia, L. J., San Roman, J. I., Calvo, J. J., and Lopez M. (1995) *Pancreas 10(1)*, 93−99.

BI980701X